JMG Online First, published on June 23, 2007 as 10.1136/jmg.2007.049510

The *C20orf133* gene is disrupted in a patient with Kabuki syndrome

Nicole MC Maas[1], Tom Van de Putte[2], Cindy Melotte[1], Annick Francis[2], Constance TRM Schrander-Stumpel[3], Damien Sanlaville[4], David Genevieve[4], Stanislas Lyonnet[4], Boyan Dimitrov[1], Koenraad Devriendt[1], Jean-Pierre Fryns[1], Joris R. Vermeesch[1]

Authors' affiliations

NMC Maas, C Melotte, B Dimitrov, K Devriendt, JP Fryns, JR Vermeesch,
Centre for Human-Genetics, University of Leuven, Leuven, Belgium

T Van de Putte, A Francis,
Laboratory of Molecular Biology (Celgen), Division Molecular and Developmental Genetics, Department of Human Genetics, KULeuven and Department of Molecular and Developmental Genetics (VIB11), Leuven, Belgium

CTRM Schrander-Stumpel,
Department of Clinical Genetics, academic hospital Maastricht and Research Institute GROW, Maastricht University, Maastricht, The Netherlands

D Sanlaville, D Genevieve, S Lyonnet,
Department of Genetics, Hôpital Necker-Enfants Malades, Assistance Publique-Hôpitaux de Paris, Paris, France

Correspondence to:
JR Vermeesch, Center for Human Genetics, Herestraat 49, 3000 Leuven, Belgium;
Joris.Vermeesch@med.kuleuven.be

ABSTRACT

Introduction: The Kabuki syndrome (KS) is a rare clinically recognizable congenital mental retardation syndrome. The aetiology of KS remains unknown.
Methods: Four carefully selected KS patients were screened for chromosomal imbalances using array comparative genomic hybridisation (CGH) at 1 Mb resolution. Mutation analysis of C10orf133, a candidate gene, was performed in 19 Kabuki patients and expression analysis of candidate gene was performed during mice development.
Results: In one patient, a 250 kb *de novo* microdeletion at 20p12.1 was detected, deleting exon 5 of *C20orf133*. The function of this gene is unknown. In situ hybridization with the mouse orthologue of *C20orf133* showed expression mainly in brain, but also in kidney, eye, inner ear, ganglia of the peripheral nervous system and lung.
Discussion: The *de novo* nature of the deletion, the expression data and the fact that *C20orf133* carries a macro domain, suggesting a role for the gene in chromatin biology, make the gene a likely candidate to cause the phenotype in this patient with KS. Both the finding of different of chromosomal rearrangements in patients with KS features and the absence of *C20orf133* mutations in 19 additional KS patients suggest that KS is genetically heterogeneous.

Key-words: Kabuki syndrome, *C20orf133*, *FLRT3*, microdeletion, array CGH

INTRODUCTION

Kabuki syndrome (KS) or Niikawa-Kuroki syndrome is a congenital mental retardation syndrome typically characterized by postnatal growth retardation, distinct facial features with long palpebral fissures and eversion of the lateral third of the lower eyelids, typical eyebrows (reminiscent of the make-up of actors of Kabuki, a traditional Japanese theatrical performance), a broad and depressed nasal tip, prominent earlobes, persistence of fetal fingertip pads, and skeletal cardiac and cleft anomalies (reviewed in [1-5]). Major malformations of the heart, kidneys and vertebra occur frequently. Psychomotoric development is almost universally present (93%), from mild moderately delayed, and severe in some patient. (Wessels et al., 2002). These individuals often are hypotonic and may manifest seizures. Endocrinological anomalies such as growth hormone deficiency and premature thelarche are observed.

The prevalence of the syndrome is estimated to be at least 1/32000 in the Japanese population,[6] and is probably similar elsewhere.[7] Up to now, no molecular cause has been determined. The sex ratio in KS is almost equal, and no increased rate of consanguinity is observed.[8] Kabuki syndrome is associated with advanced paternal age.[5] Overall, the sporadic occurrence suggests a de novo origin of autosomal dominant mutations.[6;9-13] Several persons with KS features have been published to carry a chromosome abnormality, including the sex chromosomes and various autosomes. One patient had a pericentric inversion of the Y-chromosome,[6] six had a ring chromosome X or ring Y[6;14;15] and one a 45,X karyotype.[16] The reported autosomal abnormalities include an interstitial duplication of 1p13.1p22.1,[17] a paracentric inversion of the short arm of chromosome 4,[18] partial monosomy 6q and/or partial trisomy 12q,[19] balanced translocation between 15q and 17q,[20] and pseudodicentric chromosome 13.[21] Given the incidence of heart defects, cleft palate, and the occurrence of lower lip pits in KS, microdeletions involving chromosome 22q11 and chromosome 1q32q41 have been investigated, but no association could be detected.[22;23] Bottani *et al.* (2006) excluded mutations in the *TGFβ1* and *TGFβ2* genes in KS, the motive of this study being the resemblance between the KS and the Loeys-Dietz aortic aneurysm syndrome.[24] Milunsky *et al.* (2003) reported a common 3.5 Mb duplication at 8p23.1p22 in 6 unrelated patients with KS phenotype by using conventional comparative genomic hybridization and FISH.[25] However, several follow up studies using FISH or array CGH with clones covering 8p23.1p22, entotalling the analysis of 112 patients with KS, could not confirm this duplication to be a common cause of the KS.[26-32] This multitude of reported chromosomal aberrations in KS is recognized in the variability of clinical expression of KS and its overlap with other phenotypes.

Molecular karyotyping now enables the detection of chromosomal imbalances at much higher resolution compared to conventional karyotyping. Considering the “chromosomal” phenotype, a microdeletion or microduplication would be consistent with the mostly sporadic occurrence. In this report, we studied four typical KS patients using array CGH at 1 Mb resolution and identified a putative KS causing gene in a ~250 kb region deletion.

MATERIALS AND METHODS

Patients

Given the absence of validated diagnostic criteria for KS, all patients presented in this study were selected from a larger cohort and a consensus diagnosis was established by a group of experienced clinical geneticists. Informed consent was obtained from the patients or their legal representatives. Patient DNA and leukocyte suspensions were isolated following standard protocols. Twenty KS patients were selected by clinical geneticists in respectively Leuven (four patients), Maastricht (five patients) and Paris (eleven patients).[4;27]

Patient report

The index patient with the del(20)(p12.1) has been reported before (Schrander-Stumpel *et al.*[7], patient 1). She is the second child of healthy unrelated parents, and she is currently fifteen years. She was born at 39 weeks after a delivery with forceps, with a weight of 3200 g (P50-P75) and length of 48 cm (P25-P50). A cleft palate and severe feeding problems were present. At the age of 5 months, the cleft palate was surgically closed. The feeding problems persisted though. At that time, the clinical diagnosis of KS was made. Development at age 1 year was 8 months, according to the Bayley motoric and mental scale. At 14 months, her weight and height were below the P3 (6.5 kg and 69.5 cm), her OFC was 44.2 cm (P3-P10). Development was moderately retarded. She had a premature thelarche. At 11 years secondary sexual development started and some fat deposition around the waist was evident (weight 31.6 kg (P10-P25) and height 130 cm (<P3)). Cardiac ultrasound was normal. Renal investigations revealed a left sided vesico-uretral reflux grade II and an ectopic small right kidney of 7.7 cm (located in the right hemi pelvis, (SD -2.9)). She had habitual bladder- and bowel disturbance. Ophthalmologic findings included hypermetropia, bilateral astigmatism, and alternating strabismus. Recurrent middle ear infections needed transtymponal drains. Her hands have short fifth fingers with clinodactyly, persistent fetal pads on the fingertips, and she has pedes plani. She has a short perineum, and a small urachus cyst. She is hypotonic with sialorrhoea, and has a striking muscle hypoplasia with relative subcutaneous fat excess, especially in the abdominal region. Her facial appearance is distinct, with long palpebral fissures and everted lower eyelids, a broad nasal tip, a cleft palate, oligodontia, and pre-auricular pits.

Fluorescence in situ hybridization (FISH)

FISH was performed as described before using the PAC clones 1043K1 and 375N15 at 8p to exclude duplications.[33]

Real Time quantitative PCR (qPCR)

Quantitative PCR was performed as described before.[33] Primers were designed using PrimerExpress software (Applied Biosystems) and analysed for the uniqueness of the sequence by using BLAT analysis (University of California Santa Cruz (UCSC) genome browser) and BLASTN analysis (National Center for Biotechnology Information (NCBI) database), and for repeats using RepeatMasker. (See supplementary table 1) For the selection of the primers for the exons in the QPCR technique, we used NM001033086, NM001033087, AK125899 and the VEGA transcripts of gene OTTHUMG00000031919 (this is the gene ID of C20orf133) in the Ensembl database. Quantitative PCR was performed using the Universal SYBR-green PCR master mix w/o UNG (Applied Biosystems) on the ABI7000 system (Applied Biosystems), in accordance with the manufacturer's guidelines. PCR conditions were 50°C for 2 minutes denaturation at 95°C for 10 minutes, and amplification for 40 cycles at 95°C for 15 seconds and 60°C for 1 minute. Specific PCR amplification was assessed by dissociation curve analysis. Quantification was done using the delta Ct method, and compared with the reference genes. Primers 5'-CCC-AAG-CAA-TGG-ATG-ATT-TGA-3' and 5'-GAG-CTT-CAT-CTG-GAC-CTG-GGT-3' in the tumour protein *p53* gene, 5'-CAT-CTC-ATG-GTG-GCC-CTA-GTG-3' and 5'-CTG-CTT-TGC-ATC-AAA-GAC-TGC-T-3' in the annexin A3 gene (*ANXA3*), and 5'-TTT-TCA-TTT-TCC-TGG-CCT-TGG-3' and 5'-TGA-CGG-CCA-GGA-GAA-GAC-AT-3' in the olfactory receptor, family 2, subfamily B, member 2 (*OR2B2*) gene were used as a reference for the qPCR.

Paternity testing

Paternity testing was performed by co-amplification the 17 autosomal STRs vWA (12p12-pter), D2S1338, TPOX (2p25.1-pter), D3S1338, FGA (4q28), D5S818, CSF1PO (5q33.3-34), D7S820,

D8S1179, TH01 (11p15.5), D13S317, Penta E (15q), D16S539, D18S51, D19S433, D21S11, and Penta D (21q) as described in Decorte *et al.*[34;35] The index patient and both parents were analysed. A statistical analysis was performed following procedure 'Statistical evaluation of DNA-results'. This analysis is based on the allele frequency in a Belgian and an American population (Penta A and Penta D) and an a-priori chance of 50%.

Sequence analysis

The *C20orf133* gene (AK131348) and the *FLRT3* gene (a nested gene located within intron 3 of *C20orf133)* were amplified by using primer sets for each exon (supplementary table 2) and PCR products were sequenced in both directions. Sequence analysis was performed using ABI3130 system (Applied Biosystems). (Ensembl database, release 42)

Denaturating High Performance Liquid Chromatography (DHPLC)

DHPLC analysis was performed on the Transgenomic Wave system as prescribed by the manufacturer (Transgenomic, Cheshire, UK) on genomic DNA of *C20orf133*, exon 14, using the primers 5'-TGC-ATA-TCA-CAT-TTC-TTT-TAT-TTT-TCA-3' and 5'-CCA-CGC-ACA-CAC-ACA-GGT-AT-3'. 10 µl of approximately 10ng/µl crude PCR product was loaded on a DNASep column (Transgenomic). DNA was eluted from the column by a linear acetonitrile gradient in 0.1 mM triethylamine acetate (TEAA) buffer at a constant flow rate of 1.5 ml per minute. the gradient was formed by mixing buffer A (0.1 mM TEAA) and buffer B (0.1 mM TEAA, 25% v/v acetonitrile). The temperature of the oven for optimal heteroduplex separation at partial DNA denaturation was deduced from melting profiles of the DNA sequence, obtained with the Navigator 1.6.2 software (Transgenomic). Elution patterns of patient samples were compared with those of normal control samples. The total runtime was 2.5 minutes, and gradient conditions were 52.9ºC to 62.9ºC in 2 minutes. Column temperature was 56.1ºC.[36]

Array CGH

Array CGH at 1 Mb resolution was carried out as described.[33] The chromosome 20 tiling path clone set is derived from type RP clones, plates 1 (offsets A1, A2, B1, B2) and 2 (offsets A1, A2, B1), and from CT type clones, plate 1 (offset A1). The plates were obtained from BACPAC Resource Center (Children's Hospital Oakland Research Institute Oakland, California, http://bacpac.chori.org). The hybridizations and the analyses were performed as described for 1 Mb array experiments.[37] The threshold for an abnormal intensity ratio for a deletion is the is $\log_2(3/2) - 2x$ standard deviation. The latter is the standard deviation of all intensity ratios.[37]

In situ hybridization

Mice were handled according to the guidelines of the Committee for Animal Experiments of the University of Leuven (Belgium). In situ hybridization on wild type Mus Musculus was performed at different stages of embryogenesis: E12.5, 14.5, 16.5 and 18.5. Embryos were isolated from pregnant mice and sacrificed by cervical dislocation. The day of plug detection was considered to be embryonic day (E)0.5. The embryos were fixed overnight in 4% paraformaldehyde in phosphate-buffered saline at 4°C and dehydrated in 70% ethanol before embedding in paraffin. Chromogenic ISH on 7µm thick paraffin sections was done with an antisense riboprobe labelled with digoxigenin-UTP (Roche) on the Ventana DiscoveryTM automated in situ hybridization instrument (Ventana Medical Systems, Tucson, AZ, USA) using the Ribomap and Bluemap kit (Ventana Medical Systems). A fragment containing bp 447 to 1449 of AK134694 (NCBI database) was used as template for the cRNA probe. Pre-treatment was done with the mild CC2 procedure, hybridization was at 70°C for 8 hours, post-hybridization washes were done for 32 minutes at 70°C in 0.1SSC and repeated three times. Colour development was allowed for 8 hours.

Quantitative Reverse-Transcriptase PCR (RT-PCR)

Mouse adult brain and kidney, whole E11.5 embryos, and mouse E18.5 tissues of liver, brain, lung, thymus, heart, intestine, bladder, and kidney were used for RNA extraction. RNA was extracted using the QIAquick RNA extraction kit (Qiagen), in accordance with the manufacturer's protocol. Four µg of RNA was DNase (Fermentas) treated before cDNA synthesis with SuperScript III (Invitrogen). cDNA was diluted four times for analysis. Primers were designed using PrimerExpress software (Applied Biosystems) and analysed for the uniqueness of the sequence by using BLAT analysis (University of

California Santa Cruz (UCSC) genome browser) and BLASTN analysis (National Center for Biotechnology Information (NCBI) database), and for repeats using RepeatMasker (see table 1).

Table 1 Specific clinical features in index patient with KS, phenotypic features in KS in general, and expression levels of *C20orf133* in different mouse embryonic tissues and stages.

Expression of *C20orf133* in mouse embryologic tissue	**mouse (human) developmental stage**		**Phenotypic feature in index patient with KS**	**phenotypic feature in KS**
	In situ	**Q-PCR**		
Brain: subventricular zone of striatum and olfactory lobe, the cortical plate, cerebellar primordium and the inferior colliculus of the tectum	E12.5 (6 w) +++ E18.5 (36 w) +++	E18.5 (36 w) +++ adult +++	mental retardation, neonatal hypotonia	mental retardation
Teeth: mesenchymal components of the tooth bud condensations	E14.5 (7 w) +++	n.i.	oligodontia	hypodontia, malocclusion, microdontia, small dental arches
Inner ears: cells lining the vestibule-cochlear and cochlear duct	E14.5 (7 w)	n.i.	no hearing loss	hearing loss
Eyes: cuboid epithelium of the lens and the inner nuclear layer of the retina	E16.5 (18-24w) +++	E18.5 (36w) ++	hypermetropia, bilateral astigmatism, alternating strabismus, blue sclerae, ptosis	colobomata and cataracts
Heart	E16.5 (18-24 w) +	E18.5 (36w) +	no heart defect	congenital heart disease
Kidney: tanephric glomeruli of kidney **Urinary tract** (bladder)	E14.5 (7 w) +++ E16.5 (18-24 w) +++ P0 (birth) +++	E18.5 (36w) + adult + bladder; E18.5 (36w) ++	vesico-uretral reflux grade II, ectopic small right kidney, habitual bladder disturbance	renal malformations in 28% of individuals with KS, possibly under diagnosed

+++: strong expression, ++: expression, +: low, but detectable expression, n.i.: not investigated, w: weeks, E: days post coitum, Q-PCR: quantitative PCR

RTQ-PCR was performed using qPCR MasterMix Plus for SYBR-green I w/o UNG (Eurogentec) on the ABI7500 system (Applied Biosystems), in accordance with the manufacturer's guidelines. PCR conditions were 50°C for 2 minutes, denaturation at 95°C for 10 minutes, and amplification for 40 cycles at 95°C for 15 seconds and 60°C for 1 minute. Specific PCR amplification was assessed by dissociation curve analysis. Quantification was done using the delta Ct method, and compared with the reference genes. Primers 5'-GCA-TTT-CAA-CAG-GCA-TTT-ATG-G-3' and 5'-TTA-ATC-GTA-CCT-AGG-GCA-ATG-AC-3' within the mouse homolog *AK134694* gene (UCSC genome browser) and the primers 5'-ACC-CAC-ACT-GTG-CCC-ATC-TAC-3' and 5'-AGC-CAA-GTC-CAG-ACG-CAG-G-3' in the *ß-actin* gene were designed and used as a reference for the qPCR.

Bioinformatics

Multiple alignments of amino acid sequences was performed with ClustalW (http://www.ebi.ac.uk/clustalw/) using the default parameter settings.[38] NCBI accession numbers of the sequences used for alignment are NM_080676.5 (Homo sapiens), XM_001136712.1 (Pan troglodytes), AB173156 (Macaca fascicularis), CAM14292 (Mus musculus), BC060026.1 (Xenopus laevis), and NP_956843 (Danio rerio).

RESULTS

FISH and 1 Mb array CGH results

In all patients an 8p23.1 duplication, previously suggested to be causative for the KS,[25] was excluded.([27;29] data not shown). DNA of four KS patients was hybridized using a BAC array CGH at 1 Mb resolution. For three patients, the array CGH results were normal. In a fourth patient, a $\log_2$ intensity ratio of -0,83 of one clone (RP5-855L24, 14.55-14.69 Mb) at chromosome 20, band p12.1, was observed, indicating the presence of a deletion (data not shown). FISH analysis with RP5-855L24 on metaphase spreads of the fourth patient (in this article referred to as the index patient) shows a signal on only one chromosome 20, thus confirming the presence of a deletion. (fig 1A) FISH analysis with RP5-855L24 on metaphase spreads of the parents showed a signal on both chromosomes 20 (data not shown), suggesting a *de novo* deletion. Paternity testing confirmed the father to be the biological father ($P<0.01$).

Fine mapping the size of the deletion

To refine the size of the deletion, we analysed the DNA of the index patient using the full tiling chromosome 20 array CGH. (fig 1B) Four BACs, namely CTD-2340K11 (14.52-14.66 Mb), CTD-2280K18 (14.53-14.68 Mb), CTD-2110N14 (14.53-14.65 Mb), and RP11-631F5 (14.63-14.78 Mb) have an average $\log_2$ intensity ratio of -0.78. RP11-318C17 (14.76-14.93 Mb) has a $\log_2$ intensity ration of -0.55, while RP11-582I19 (14.43-14.59 Mb) and RP11-224A21 (14.83-15.01 Mb) show normal intensity ratios. FISH using RP11-318C17 expressed a normal signal on the normal chromosome 20 and a weak signal on a second chromosome 20, indicating that this clone was partially deleted. Taken together, the deletion spans about 250 kb. Recently, large scale benign copy number variations (CNVs) have been detected in the human population.[39] To assure that the *de novo* deletion in our patient is not a benign CNV, both the database of genomic variants and the genomic variation in 270 HapMap families (Redon track, Ensembl release 42, Dec 2006) were inquired. The deletion is not a known benign variant.[39;40]

C20orf133 as a candidate gene for KS

The deletion in the DNA of the index patient is located within *C20orf133*, (or AK131348 from the NITE Biological Resource Centre, or GC20P013971). The gene contains 17 exons and spans 2.06 Mb located at 13.92 Mb to 15.98 Mb. The gene structure of *C20orf133* and the putative protein encoded by it is evolutionary conserved. In particular, the N-terminal half of the putative protein is highly conserved amongst species: From amino acid 1 to 243 (of a total of 425 amino acids), the human protein shows ≥96% similarity with the Pan troglodytes, Macaca fascicularis, and Mus musculus, and respectively 84% and 79% with the Xenopus laevis and Danio rerio orthologues. This part of the protein contains an Appr-1-P processing domain, belonging to the macro domain family. The macro domain is described in approximately 300 of the proteins stored in the SMART (Simple Modular Architecture Research Tool) database. The C-terminal region of the protein is less conserved: similarity with Pan troglodytes is still 98%, but drops down to 76% when comparing the putative human protein with Macaca fascicularis, 57% with Mus musculus, and only 33% and 32% with the Danio rerio and Xenopus laevis orthologues respectively.[38] The DNA of the index patient shows, together with intronic sequences, a deletion of the entire exon 5 of this gene. This exon is located within the N-terminally conserved region (fig 2B) and encompasses 117 nucleotides, thus removing 39 aminoacids from the patients protein but not causing a frame shift downstream (fig 2A, 2B). *C20orf133* (Unigene cluster name Hs.570367) mRNA has been shown to be expressed in fetal and adult human brain, thymus, skeletal muscle, liver, pancreas, prostate, kidney and lung (UCSC genome browser and GenCards®: Unigene Electronic Northern blot results).

Expression pattern of C20orf133 in the mouse embryo

In order to gain insight in the relations of this gene with the patients' phenotype, the expression of the mouse orthologue of *C20orf133* mRNA was studied using in situ hybridization with an AK134694 cDNA riboprobe (NITE Biological Resource Centre) in wild-type fetuses at different stages of embryonic development. At E12.5, significant expression levels were observed in the neural tube and in the ganglia of the peripheral nervous system: the dorsal root and cranial ganglia (fig 3A and data not shown). At developmental stage E14.5, a high expression level was found in the metanephric glomeruli of the kidney, whereas the medullary region was devoid of mRNA. (fig 3B) In addition, this gene was found to be expressed in the epithelium lining the lumen of the gut and stomach, the seminiferous tubules, the lungs, the dorsal root ganglia and spinal cord (data not shown). In the cranial region, elevated levels of *C20orf133* expression were seen in the epithelial and mesenchymal components of the tooth bud condensations, the epithelium of the primitive nasal cavity, in cells lining the vestibulo-cochlear and cochlear duct and the cranial ganglia (fig 3C and data not shown). In the E16.5 embryo, the lung and kidney maintain *C20orf133* expression. Specific hybridization was also detected in the papilla of the whisker follicles. In the eye, strong in situ staining is observed in the cuboid epithelium of the lens and the inner nuclear (neuroblastic) layer of the retina (fig 3D and data not shown). Also the brain, and in particular the ventricular zone, which is also seen in the neural tube, becomes positive for *C20orf133* mRNA at this developmental stage (fig 3E). The expression in the brain is also clear at E18. Expression in the myocardium of the heart was observed at developmental stage E16.5 (data not shown). Just before birth, at E18.5, *C20orf133* remains expressed the brain, with relatively high levels of expression in discrete regions: the subventricular zone of striatum and olfactory lobe, the cortical plate, cerebellar primordium and the inferior colliculus of the tectum (fig 3G). In P0 kidney, expression of *C20orf133* expression is maintained in the methanephric glomeruli whereas it is not detectable in the adrenal gland (fig 3F).

The presence and level of expression of *C20orf133* mRNA was also monitored using RT-PCR on multiple tissues and at different embryonic stages. mRNA of a whole E11.5 embryos, mRNA of liver, eye, brain, lung, thymus, heart, intestine, bladder, and kidney at stage E18.5 and mRNA of adult kidney and adult brain were used. High expression was observed in stage E18.5 and adult brain. Low, but significant expression levels were observed in the E11.5 embryo, kidneys of embryonic stage E18.5 and of adult mice and E18.5 eyes, and bladder. Expression observed in the heart at stage E18.5 had 45 times lower expression than in the brain at stage E18.5.

Mutation screening in other KS patients

We investigated whether other KS patients carried either deletions or point mutations in *C20orf133*. FISH analysis using RP5-855L24 as a probe on metaphase spreads of 14 from the 19 other KS patients was performed and no deletion was detected. In the 5 patients from Maastricht, no metaphase spreads were available. Full tiling chromosome 20 array CGH was performed on the DNA of 5 KS patients from Maastricht and on the 3 other patients from Leuven. There was not sufficient DNA from the Paris group to perform these analyses. No imbalances were detected. To exclude other mutations in the coding sequence, all *C20orf133* exons and their intron-exon boundaries were sequenced on genomic DNA of the other 19 KS patients. A single base pair replacement (SNP) in exon 14 (c.19C>T) was detected in 7 patients. This SNP is not present in the HUGO SNP database. To determine whether the SNP would be a common polymorphism, DHPLC was performed on 82 control DNA samples (164 alleles). The SNP was found to be heterozygous in 25 controls, and 3 controls were homozygous for the base pair substitution. Hence, we conclude that the SNP is a benign polymorphism. Since sequencing analysis may not detect whole exon deletions or duplications and which may be small enough to be below the detection limit of the current CGH array, we performed exon-specific qPCR on the available genomic DNA of the 9 patients screened with the tiling array of chromosome 20. This approach confirmed the deletion of exon 5 in the index patient, but no other deletions or duplications were detected in the other 9 patients.

Mutation analysis in FLRT3

Since genomic rearrangements, and thus deletions, can influence the expression of nearby located genes, the effect of the detected microdeletion in the index patient might be indirect, disturbing gene function(s) in the proximity. Because neither pointmutations nor deletions of the *C20orf133* gene were detected in the remaining KS patients, we investigated whether FLRT3, a nested gene located within intron 3 of the *C20orf133*, could be affected. FLRT3, (fibronectin-like domain-containing leucine-rich transmembrane protein 3) is a transmembrane modulator of FGF-MAPK signalling in vertebrates and may be involved in receptor signalling protein activity, transferase activity and cell adhesion. However,

neither deletions nor duplications were detected in the clones covering FLRT3 in the 9 KS patients screened using the chromosome 20 full tiling path array. Subsequently, the 3 FLRT3 exons and their intron-exon boundaries were sequenced in the DNA of all 20 KS patients, and no mutation was detected.

DISCUSSION

We report a *de novo* microdeletion of ~250 kb at 20p12.1 in a 15 year old girl with the KS, using array CGH with a 1Mb resolution. This is a fortunate finding, since the resolution of the array is lower that the deletion size. Several observations suggests that *C20orf133* is a causative gene for the observed phenotype in the index patient. First, the deletion in this patient occurred *de novo* in the macro-appr-pase-like domain of the putative protein, thereby likely disrupting the enzymatic activity. Second, the expression pattern of the *C20orf133* gene during mouse embryonic development supports its importance in the development of different tissues and organs affected in this patient. The gene contains a macro functional domain, which ties it with chromatin structure. Recently, multiple congenital malformation syndromes have been described to be caused by haploinsufficiency of a gene involved in chromatin remodeling.[41-46]

In Mus Musculus, both in situ hybridization and RT-PCR showed that *C20orf133* is expressed during embryonic development of the brain, in particular the ventricular zone. Just before birth, at E18.5, *C20orf133* remains expressed in the brain, with relatively high levels of expression in discrete regions: the subventricular zone of striatum and olfactory lobe, the cortical plate, cerebellar primordium and the inferior colliculus of the tectum. The high levels of expression in the brain across a wide range of developmental stages and its persistence during adulthood is consistent with a role for the gene in mental development and may reflect a requirement for *C20orf133* in axonal outgrowth and functioning of the adult cortex. The gene is also expressed in other embryonic tissues that are typically affected in Kabuki patients. High levels of expression in embryonic kidney/urinary tract were detected. Renal malformations were observed in 28% of the individuals with KS,[47] but might be under diagnosed since they sometimes remain asymptomatic. Expression was observed in several craniofacial regions, which, given the specific facial characteristics of KS patients, can be expected. *C20orf133* is expressed in the mesenchymal components of the tooth bud condensations at E14.5. Interestingly, dental anomalies such as hypodontia, malocclusion, microdontia and small dental arches, are seen in 68% of KS patients.[47;48] Expression of the gene in the cells lining the vestibule-cochlear and cochlear duct at stage E14.5, possibly explaining hearing loss reported in up to 82% of KS patients.[47] In the developing mouse eye, strong hybridization was observed in the cuboid epithelium of the lens and the inner nuclear layer of the retina which could explain the occurrence of colobomata and cataracts in KS.[3] Expression in the heart is low, despite the CHD reported in 42% of KS patients[47]. Interestingly, in the index patient no heart defect was observed after physical and ultrasound investigation. An overview of mice expression data, the phenotype of the index patient and the Kabuki syndrome features are provided in table 1.

The *C20orf133* gene contains a macro domain (http://www.ncbi.nlm.nih.gov/IEB/Research/Acembly/). Previously identified as displaying an Appr-1"-P (ADP-ribose-1"-monophosphate) processing activity, the macro domain may play roles in distinct ADP-ribose pathways. *In vivo* evidence suggests that ADP-ribosylation is an important post-translational modification which plays a role in DNA repair, transcriptional activation and repression, telomere and chromatin biology, long-term memory formation, DNA binding and DNA and/or RNA unwinding, among other processes.[49] Thus far, no macro domain containing genes have been implemented in mental retardation and/or developmental delay. However, it is striking that several syndromes with mental retardation and multiple congenital anomalies result from haploinsufficiency of genes involved in DNA repair, transcription, chromatin biology and long term memory formation, exactly the same processes in which macro domain containing proteins are known to play a role. Possibly, the macro domain family of proteins may represent a novel class of dosage sensitive genes that may cause developmental disorders when mutated.

Genevieve *et al.* describe one of the KS patients in their study with a clinical overlap with CHARGE syndrome.[50] This syndrome was recently shown to be caused by mutations in or deletions of *CHD7*, a member of the chromodomain helicase DNA-binding (CHD) genes, which have a unique combination of functional domains, including two N-terminal chromodomains, a SNF2-like ATPase/helicase domain and a DNA-binding domain.[51] ADP-ribose binding affects the function of the Alc1 protein, a protein with homology to the Snf2 ATPase/helicase.[52] Therefore, the alteration of the phosphorylation-status of the ADP-ribose by *C20orf133* may have an influence on the activity of

this Swi/Snf chromatin remodeling factor and as such explain the clinical overlap between some patients with CHARGE syndrome and Kabuki syndrome.

Screening for mutations, deletions or duplications in 20 other KS patients did not reveal any mutations within the *C20orf133* candidate gene. Possibly, mutations outside the coding region as well as epigenetic changes might cause the Kabuki phenotype. Also, we cannot exclude the presence of as yet unknown genes within the region which might be affected by this deletion. . However, it seems likely that KS is genetically heterogeneous and that mutations in other genes may result in phenocopies. The accumulating findings of several different chromosomal rearrangements in KS patients summarized above may pinpoint several loci that may cause KS.

Recently, other syndromes associated with multiple congenital anomalies and mental retardation have been shown to be genetically heterogeneous. For example, the Noonan syndrome can be caused by mutations in the protein-tyrosine phosphatase nonreceptor-type 11 (*PTPN11*),[42] or by mutations in the V-Ki-Ras2 Kirsten rat sarcoma 2 viral oncogene homolog (*KRAS2*),[45] both components of the Ras pathway, or by mutations in the Son of Sevenless Drosophila homolog 1 gene (*SOS1*).[46] The CHARGE syndrome phenotype can, in addition to mutations in the *CHD7* gene, also be caused by a mutation in the semaphoring-3E gene (*SEMA3E*).[43] The Rubinstein-Taybi syndrome can be caused by mutations in the gene encoding the transcriptional coactivator CREB-binding protein (*CREBBP*)[41] or by mutations in the E1A-binding protein 300-KD (*EP300*) gene.[44]

In conclusion, the *C20orf133* is a good candidate gene for causing the phenotype in the index patient. Further evaluation is needed to determine to what extent this gene could be involved in the etiology of KS. In addition, this study further illustrates the value of array CGH to localize genes causing developmental disorders. The fortuitous finding of a microdeletion below the 1 Mb resolution of our array demonstrates that high resolution array CGH will enable the functional identification of more genes involved in the etiology of KS and other clinical genetic syndromes.

ACKNOWLEDGMENTS

We wish to thank the MicroArray Facility, Flanders Interuniversity Institute for Biotechnology (VIB) for their help in the spotting of the arrays and the Mapping Core and Map Finishing groups of the Wellcome Trust Sanger Institute for the initial clone supply and verification. This work was made possible by grants OT/O2/40, GOA/2006/12 and Centre of Excellence SymBioSys (Research Council K.U.Leuven EF/05/007), Catholic University of Leuven. We wish to thank Mrs. R. Thoelen for her technical support in FISH analyses, and dr. E. Schollen for her help in the performance of the DHPLC and dr. K. Martens for his contribution to this article. We are also indebted to Prof. D. Huylebroeck for support and expert discussion.

FIGURE LEGENDS

Figure 1A FISH using Spectrum orange labelled RP5-855L24. The bold arrow indicates the normal chromosome 20, the thin arrow indicates the derivative chromosome 20. **B:** Full tiling chromosome 20 array ratio profiles using DNA from a patient with a deletion and a reference DNA from a normal individual. The X-axis represents the clones ordered from the 20p to the 20q telomere according to their clone position in the February 2004 Ensembl freeze. The Y-axis marks the hybridization ratio plotted on a $\log_2$ scale.

Figure 2A Schematic view of the exons and introns of the gene *C20orf133* and FLRT3 at a genomic level, designed using Vector NTi10. *C20orf133* contains 17 exons, and is 2054882 bp in size. FLRT3 contains 3 exons, is 13621 bp, in size, and is in reverse direction with *C20orf133*. The red line indicates the deletion of the index patient. The scale is indicated in kilo basepairs. **B:** Multiple alignment of the *C20orf133* protein between Homo sapiens, Pan troglodytes (chimpanzee), Macaca fascicularis, Mus musculus, Xenopus laevis, and Danio rerio. The red line indicates the macro-Appr-pase-like domain. The green line indicates the deletion region of the index patient.

Figure 3 The embryonic expression pattern of the mouse orthologue of *C20orf133* (AK134694). **A:** Sagittal section of an E8.5 embryo within the deciduum (decid) reveals a widespread gene expression in all intra- and extra-embryonic tissues. The decidual tissue surrounding the embryo is largely devoid of *C20orf133* mRNA **B:** Transversal section (at the level of the thorax) through an E12.5 embryo

showing the spinal cord and the dorsal root ganglia (DRG) reveals a particular high expression of the mouse orthologue of *C20orf133* (AK134694) in the condensed DRG (red arrowhead). Lower, but still significant expression levels can be detected in the neural tube, in particular in the ventricular zone (VZ). **C:** Transversal section through E14.5 kidneys reveals a high *in situ* signal. **D:** Cranial section at E14.5. High mRNA content is visualized in cells lining the vestibule-cochlear and cochlear duct and in the cranial ganglia. **E:** In the E16.5 eye strong *in situ* staining is observed in the cuboid epithelium of the lens and the inner nuclear (neuroblastic) layer of the retina. **F:** *In situ* staining on a kidney of a newborn (P0) mouse demonstrates significant expression of the mouse *C20orf133* orthologue in the kidney whereas the adrenal gland lacks detectable expression levels. **G:** Sagittal section through an E18.5 brain reveals expression throughout the brain, with particularly high levels of expression in the subventricular zone of the striatum and olfactory lobe, the cortical plate, cerebellar primordium and the inferior colliculus of the tectum. (BA: branchial arch, som: somites, nt: neural tube, decid: deciduum).

REFERENCES

1 Donadio A, Garavelli L, Banchini G, Neri G. Kabuki syndrome and diaphragmatic defects: a frequent association in non-Asian patients? *Am J Med Genet* 2000;**91**:164-5.
2 White SM, Thompson EM, Kidd A, Savarirayan R, Turner A, Amor D, Delatycki MB, Fahey M, Baxendale A, White S, Haan E, Gibson K, Halliday JL, Bankier A. Growth, behavior, and clinical findings in 27 patients with Kabuki (Niikawa-Kuroki) syndrome. *Am J Med Genet A* 2004;**127**:118-27.
3 Adam MP, Hudgins L. Kabuki syndrome: a review. *Clin Genet* 2005;**67**:209-19.
4 Schrander-Stumpel CT, Spruyt L, Curfs LM, Defloor T, Schrander JJ. Kabuki syndrome: Clinical data in 20 patients, literature review, and further guidelines for preventive management. *Am J Med Genet A* 2005;**132**:234-43.
5 Armstrong L, Abd El Moneim A, Aleck K, Aughton DJ, Baumann C, Braddock SR, Gillessen-Kaesbach G, Graham JM, Jr., Grebe TA, Gripp KW, Hall BD, Hennekam R, Hunter A, Keppler-Noreuil K, Lacombe D, Lin AE, Ming JE, Kokitsu-Nakata NM, Nikkel SM, Philip N, Raas-Rothschild A, Sommer A, Verloes A, Walter C, Wieczorek D, Williams MS, Zackai E, Allanson JE. Further delineation of Kabuki syndrome in 48 well-defined new individuals. *Am J Med Genet A* 2005;**132**:265-72.
6 Niikawa N, Kuroki Y, Kajii T, Matsuura N, Ishikiriyama S, Tonoki H, Ishikawa N, Yamada Y, Fujita M, Umemoto H, et al. Kabuki make-up (Niikawa-Kuroki) syndrome: a study of 62 patients. *Am J Med Genet* 1988;**31**:565-89.
7 Schrander-Stumpel C, Meinecke P, Wilson G, Gillessen-Kaesbach G, Tinschert S, Konig R, Philip N, Rizzo R, Schrander J, Pfeiffer L, et al. The Kabuki (Niikawa-Kuroki) syndrome: further delineation of the phenotype in 29 non-Japanese patients. *Eur J Pediatr* 1994;**153**:438-45.
8 Lerone M, Priolo M, Naselli A, Vignolo M, Romeo G, Silengo MC. Ectodermal abnormalities in Kabuki syndrome. *Am J Med Genet* 1997;**73**:263-6.
9 Courtens W, Rassart A, Stene JJ, Vamos E. Further evidence for autosomal dominant inheritance and ectodermal abnormalities in Kabuki syndrome. *Am J Med Genet* 2000;**93**:244-9.
10 Halal F, Gledhill R, Dudkiewicz A. Autosomal dominant inheritance of the Kabuki make-up (Niikawa-Kuroki) syndrome. *Am J Med Genet* 1989;**33**:376-81.
11 Ilyina H, Lurie I, Naumtchik I, Amoashy D, Stephanenko G, Fedotov V, Kostjuk A. Kabuki make-up (Niikawa-Kuroki) syndrome in the Byelorussian register of congenital malformations: ten new observations. *Am J Med Genet* 1995;**56**:127-31.
12 Shotelersuk V, Punyashthiti R, Srivuthana S, Wacharasindhu S. Kabuki syndrome: report of six Thai children and further phenotypic and genetic delineation. *Am J Med Genet* 2002;**110**:384-90.
13 Silengo M, Lerone M, Seri M, Romeo G. Inheritance of Niikawa-Kuroki (Kabuki makeup) syndrome. *Am J Med Genet* 1996;**66**:368.
14 Dennis NR, Collins AL, Crolla JA, Cockwell AE, Fisher AM, Jacobs PA. Three patients with ring (X) chromosomes and a severe phenotype. *J Med Genet* 1993;**30**:482-6.
15 McGinniss MJ, Brown DH, Burke LW, Mascarello JT, Jones MC. Ring chromosome X in a child with manifestations of Kabuki syndrome. *Am J Med Genet* 1997;**70**:37-42.
16 Wellesley DG, Slaney S. Kabuki make-up and Turner syndromes in the same patient. *Clin Dysmorphol* 1994;**3**:297-300.
17 Lo IF, Cheung LY, Ng AY, Lam ST. Interstitial Dup(1p) with findings of Kabuki make-up syndrome. *Am J Med Genet* 1998;**78**:55-7.

18 Fryns JP, Van den Berghe H, Schrander-Stumpel C. Kabuki (Niikawa-Kuroki) syndrome and paracentric inversion of the short arm of chromosome 4. *Am J Med Genet* 1994;**53**:204-5.
19 Jardine PE, Burvill-Holmes LC, Schutt WH, Lunt PW. Partial 6q monosomy/partial 12q trisomy in a child with features of Kabuki make-up syndrome. *Clin Dysmorphol* 1993;**2**:269-73.
20 Galan-Gomez E, Cardesa-Garcia JJ, Campo-Sampedro FM, Salamanca-Maesso C, Martinez-Frias ML, Frias JL. Kabuki make-up (Niikawa-Kuroki) syndrome in five Spanish children. *Am J Med Genet* 1995;**59**:276-82.
21 Lynch SA, Ashcroft KA, Zwolinski S, Clarke C, Burn J. Kabuki syndrome-like features in monozygotic twin boys with a pseudodicentric chromosome 13. *J Med Genet* 1995;**32**:227-30.
22 Li M, Zackai EH, Niikawa N, Kaplan P, Driscoll DA. Kabuki syndrome is not caused by a microdeletion in the DiGeorge/velocardiofacial chromosomal region within 22q 11.2. *Am J Med Genet* 1996;**65**:101-3.
23 Makita Y, Yamada K, Miyamoto A, Okuno A, Niikawa N. Kabuki make-up syndrome is not caused by microdeletion close to the van der Woude syndrome critical region at 1q32-q41. *Am J Med Genet* 1999;**86**:285-8.
24 Bottani A, Pardo B, Bouchardy I, Schoumans J, Toutain A, Conrad B. No major contribution of the TGFBR1- and TGFBR2-mediated pathway to Kabuki syndrome. *Am J Med Genet A* 2006;**140**:903-5.
25 Milunsky JM, Huang XL. Unmasking Kabuki syndrome: chromosome 8p22-8p23.1 duplication revealed by comparative genomic hybridization and BAC-FISH. *Clin Genet* 2003;**64**:509-16.
26 Miyake N, Harada N, Shimokawa O, Ohashi H, Kurosawa K, Matsumoto T, Fukushima Y, Nagai T, Shotelersuk V, Yoshiura K, Ohta T, Kishino T, Niikawa N, Matsumoto N. On the reported 8p22-p23.1 duplication in Kabuki make-up syndrome (KMS) and its absence in patients with typical KMS. *Am J Med Genet A* 2004;**128**:170-2.
27 Engelen JJ, Loneus WH, Vaes-Peeters G, Schrander-Stumpel CT. Kabuki syndrome is not caused by an 8p duplication: a cytogenetic study in 20 patients. *Am J Med Genet A* 2005;**132**:276-7.
28 Hoffman JD, Zhang Y, Greshock J, Ciprero KL, Emanuel BS, Zackai EH, Weber BL, Ming JE. Array based CGH and FISH fail to confirm duplication of 8p22-p23.1 in association with Kabuki syndrome. *J Med Genet* 2005;**42**:49-53.
29 Sanlaville D, Genevieve D, Bernardin C, Amiel J, Baumann C, de Blois MC, Cormier-Daire V, Gerard B, Gerard M, Le Merrer M, Parent P, Prieur F, Prieur M, Raoul O, Toutain A, Verloes A, Viot G, Romana S, Munnich A, Lyonnet S, Vekemans M, Turleau C. Failure to detect an 8p22-8p23.1 duplication in patients with Kabuki (Niikawa-Kuroki) syndrome. *Eur J Hum Genet* 2005;**13**:690-3.
30 Schoumans J, Nordgren A, Ruivenkamp C, Brondum-Nielsen K, Teh BT, Anneren G, Holmberg E, Nordenskjold M, Anderlid BM. Genome-wide screening using array-CGH does not reveal microdeletions/microduplications in children with Kabuki syndrome. *Eur J Hum Genet* 2005;**13**:260-3.
31 Turner C, Lachlan K, Amerasinghe N, Hodgkins P, Maloney V, Barber J, Temple IK. Kabuki syndrome: new ocular findings but no evidence of 8p22-p23.1 duplications in a clinically defined cohort. *Eur J Hum Genet* 2005;**13**:716-20.
32 Kimberley KW, Morris CA, Hobart HH. BAC-FISH refutes report of an 8p22-8p23.1 inversion or duplication in 8 patients with Kabuki syndrome. *BMC Med Genet* 2006;**7**:46.
33 Menten B, Maas N, Thienpont B, Buysse K, Vandesompele J, Melotte C, de Ravel T, Van Vooren S, Balikova I, Backx L, Janssens S, De Paepe A, De Moor B, Moreau Y, Marynen P, Fryns JP, Mortier G, Devriendt K, Speleman F, Vermeesch JR. Emerging patterns of cryptic chromosomal imbalance in patients with idiopathic mental retardation and multiple congenital anomalies: a new series of 140 patients and review of published reports. *J Med Genet* 2006;**43**:625-33.
34 Decorte R, Engelen M, Larno L, Nelissen K, Gilissen A, Cassiman JJ. Belgian population data for 15 STR loci (AmpFlSTR SGM Plus and AmpFlSTR profiler PCR amplification kit). *Forensic Sci Int* 2004;**139**:211-3.
35 Decorte R, Verhoeven E, Vanhoutte E, Knaepen K, Cassiman JJ. Allele frequency data for 19 short tandem repeats (PowerPlex 16 and FFFl) in a Belgian population sample. *J Forensic Sci* 2006;**51**:436-7.
36 Schollen E, Martens K, Geuzens E, Matthijs G. DHPLC analysis as a platform for molecular diagnosis of congenital disorders of glycosylation (CDG). *Eur J Hum Genet* 2002;**10**:643-8.
37 Vermeesch JR, Melotte C, Froyen G, Van Vooren S, Dutta B, Maas N, Vermeulen S, Menten B, Speleman F, De Moor B, Van Hummelen P, Marynen P, Fryns JP, Devriendt K. Molecular karyotyping: array CGH quality criteria for constitutional genetic diagnosis. *J Histochem Cytochem* 2005;**53**:413-22.

38 Thompson JD, Higgins DG, Gibson TJ. CLUSTAL W: improving the sensitivity of progressive multiple sequence alignment through sequence weighting, position-specific gap penalties and weight matrix choice. *Nucleic Acids Res* 1994;**22**:4673-80.
39 Redon R, Ishikawa S, Fitch KR, Feuk L, Perry GH, Andrews TD, Fiegler H, Shapero MH, Carson AR, Chen W, Cho EK, Dallaire S, Freeman JL, Gonzalez JR, Gratacos M, Huang J, Kalaitzopoulos D, Komura D, MacDonald JR, Marshall CR, Mei R, Montgomery L, Nishimura K, Okamura K, Shen F, Somerville MJ, Tchinda J, Valsesia A, Woodwark C, Yang F, Zhang J, Zerjal T, Armengol L, Conrad DF, Estivill X, Tyler-Smith C, Carter NP, Aburatani H, Lee C, Jones KW, Scherer SW, Hurles ME. Global variation in copy number in the human genome. *Nature* 2006;**444**:444-54.
40 Simon-Sanchez J, Scholz S, Fung HC, Matarin M, Hernandez D, Gibbs JR, Britton A, de Vrieze FW, Peckham E, Gwinn-Hardy K, Crawley A, Keen JC, Nash J, Borgaonkar D, Hardy J, Singleton A. Genome-wide SNP assay reveals structural genomic variation, extended homozygosity and cell-line induced alterations in normal individuals. *Hum Mol Genet* 2007;**16**:1-14.
41 Petrij F, Giles RH, Dauwerse HG, Saris JJ, Hennekam RC, Masuno M, Tommerup N, van Ommen GJ, Goodman RH, Peters DJ, et al. Rubinstein-Taybi syndrome caused by mutations in the transcriptional co-activator CBP. *Nature* 1995;**376**:348-51.
42 Tartaglia M, Mehler EL, Goldberg R, Zampino G, Brunner HG, Kremer H, van der Burgt I, Crosby AH, Ion A, Jeffery S, Kalidas K, Patton MA, Kucherlapati RS, Gelb BD. Mutations in PTPN11, encoding the protein tyrosine phosphatase SHP-2, cause Noonan syndrome. *Nat Genet* 2001;**29**:465-8.
43 Lalani SR, Safiullah AM, Molinari LM, Fernbach SD, Martin DM, Belmont JW. SEMA3E mutation in a patient with CHARGE syndrome. *J Med Genet* 2004;**41**:e94.
44 Roelfsema JH, White SJ, Ariyurek Y, Bartholdi D, Niedrist D, Papadia F, Bacino CA, den Dunnen JT, van Ommen GJ, Breuning MH, Hennekam RC, Peters DJ. Genetic heterogeneity in Rubinstein-Taybi syndrome: mutations in both the CBP and EP300 genes cause disease. *Am J Hum Genet* 2005;**76**:572-80.
45 Schubbert S, Zenker M, Rowe SL, Boll S, Klein C, Bollag G, van der Burgt I, Musante L, Kalscheuer V, Wehner LE, Nguyen H, West B, Zhang KY, Sistermans E, Rauch A, Niemeyer CM, Shannon K, Kratz CP. Germline KRAS mutations cause Noonan syndrome. *Nat Genet* 2006;**38**:331-6.
46 Shannon K, Bollag G. Sending out an SOS. *Nat Genet* 2007;**39**:8-9.
47 Matsumoto N, Niikawa N. Kabuki make-up syndrome: a review. *Am J Med Genet C Semin Med Genet* 2003;**117**:57-65.
48 Matsune K, Shimizu T, Tohma T, Asada Y, Ohashi H, Maeda T. Craniofacial and dental characteristics of Kabuki syndrome. *Am J Med Genet* 2001;**98**:185-90.
49 Seman M, Adriouch S, Haag F, Koch-Nolte F. Ecto-ADP-ribosyltransferases (ARTs): emerging actors in cell communication and signaling. *Curr Med Chem* 2004;**11**:857-72.
50 Genevieve D, Amiel J, Viot G, Le Merrer M, Sanlaville D, Urtizberea A, Gerard M, Munnich A, Cormier-Daire V, Lyonnet S. Atypical findings in Kabuki syndrome: report of 8 patients in a series of 20 and review of the literature. *Am J Med Genet A* 2004;**129**:64-8.
51 Sanlaville D, Etchevers HC, Gonzales M, Martinovic J, Clement-Ziza M, Delezoide AL, Aubry MC, Pelet A, Chemouny S, Cruaud C, Audollent S, Esculpavit C, Goudefroye G, Ozilou C, Fredouille C, Joye N, Morichon-Delvallez N, Dumez Y, Weissenbach J, Munnich A, Amiel J, Encha-Razavi F, Lyonnet S, Vekemans M, Attie-Bitach T. Phenotypic spectrum of CHARGE syndrome in fetuses with CHD7 truncating mutations correlates with expression during human development. *J Med Genet* 2006;**43**:211-7.
52 Karras GI, Kustatscher G, Buhecha HR, Allen MD, Pugieux C, Sait F, Bycroft M, Ladurner AG. The macro domain is an ADP-ribose binding module. *Embo J* 2005;**24**:1911-20.

Supplemental Table 1 Primers used for copy number variation screening of exons of the C20orf133 gene by means of qPCR.

Gene, exon	**Sequence 5' to 3'**
C20orf133, exon 1 forward	ACA CAC CCT GTT TGC CCG T
C20orf133, exon 1 reverse	GGC TGG CTT TAA GCT GCA AGT
C20orf133, exon 2 forward	AGA GAC TAT ATT CCC CTG AAC AGC A
C20orf133, exon 2 reverse	CTT CAT CTC CTC CTT CCA TGA TAG A
C20orf133, exon 3 forward	AAG AAA ATA CTC AGG AAA CAT CCC A
C20orf133, exon 3 reverse	CTT TTT CAG TCA AAC TTT TCT TCA CCT
C20orf133, exon 4 forward	TTT AAA CAG CAA ATG CCA GTC TTC
C20orf133, exon 4 reverse	TTC AGG ACT TAC CAC CTC CTC C
C20orf133, exon 5 forward	TAT TCA TAG AGC AGC CGG CC
C20orf133, exon 5 reverse	TTC AGG TTA CGA CAT TCA GCT AGC
C20orf133, exon 6 forward	CTG TAG GGC CAA TAG CCA GG
C20orf133, exon 6 reverse	GGT CTT CCT TGT GGG AAC CAT
C20orf133, exon 7 forward	TTC ATT GTT ATT TTT GTG GTT TAT TCA CA
C20orf133, exon 7 reverse	TGT TGA GAT GCA GGG AAA TGC
C20orf133, exon 8 forward	TCT AGG CTT TCC CAA CGA GC
C20orf133, exon 8 reverse	TTA ATG GTG TTG AGG GCA ATG A
C20orf133, exon 9 forward	CGG ATC ATT TTC TGT GTC TTC TTA GA
C20orf133, exon 9 reverse	TCA TTT TCT TTT TGT AGA TTT TGA AGT CA
C20orf133, exon 10 forward	GAT AAT AAT GAA GAA GAA GAG GAT GTT GAA
C20orf133, exon 10 reverse	AAA AGT ATG AAT TTA ATA CCT GAA TCT TCT TTC
C20orf133, exon 11 forward	AAC GGT CCA GAG GAG AAG CAA
C20orf133, exon 11 reverse	TTG GCT CTG CTC TTC CAT TTC
C20orf133, exon 12 forward	TTT CTG CTT TAT AGA TGG TGT CAA CA
C20orf133, exon 12 reverse	CAG TCT TCA ACT GCC TCT TCT GAA
C20orf133, exon 13 forward	GAA AAT ATT ACA AAA GGC GGT GAA G
C20orf133, exon 13 reverse	TTG GTC ACG CAC AGA ATG ATC T
C20orf133, exon 14 forward	TCA CTG TTT TGA ACA GGA CAA GAG A
C20orf133, exon 14 reverse	GTT TCA ATT TTT ATT TCA TTC TTC GTT G
C20orf133, exon 15 forward	AGA TGC CGT GAT TGT GGA GC
C20orf133, exon 15 reverse	TGG TCC TCT GTT AAT GGA ATC ACT T
C20orf133, exon 16 forward	GAG GAC ACA CCT AGG ATG CCT G
C20orf133, exon 16 reverse	TTCT AGG TCA CTG GAG CCT TCA C
C20orf133, exon 17 forward	TGC AGA GGC ATA ACA GAA GGG
C20orf133, exon 17 reverse	GGA AGA GAC CCA GAT GGC TG

Supplemental Table 2 Primers used for sequencing analysis at the C20orf133 and FLRT3 locus.

Gene, exon	**Sequence 5' to 3'**
C20orf133, exon 1 forward	CAG CTC CCT AGC GTC GTC
C20orf133, exon 1 reverse	GGC ACA CAC AGC CTG ACC
C20orf133, exon 2 forward	GGA-GTC-ACT-GGA-TTT-GCA-TTG-TG
C20orf133, exon 2 reverse	CCA-CCA-AAG-CAG-CAA-ATC-TCT-AA
C20orf133, exon 3 forward	GAG-CAT-GAC-ACA-TAT-TGG-GTC-TTG
C20orf133, exon 3 reverse	CCT-AAT-CTC-AAC-CTA-GCG-CCT-TTC
C20orf133, exon 4 forward	CAG GCT GTC TTT AAA TGA AAG TAA AT
C20orf133, exon 4 reverse	TTG TAA TTG ATG ACT ACA GCA AAA T
C20orf133, exon 5 forward	GCT-AGT-GTT-TGA-AAC-ATT-GGA-CAC-C
C20orf133, exon 5 reverse	CCA-CTG-CCA-TTT-CCT-TTT-CCA-GTT-A
C20orf133, exon 6 forward	GTC GCC AAT GTA TTG CTT AGC
C20orf133, exon 6 reverse	CCT ACC TCT CTT TAG ACA AGA CAG A
C20orf133, exon 7 forward	CAG TGT CCC CTA CTC CAA CTC AT
C20orf133, exon 7 reverse	CCC AAA AGA ATC TGA ATA GCC TC
C20orf133, exon 8 forward	TCA TAT CCA TGT ACA TCT TAC TGA GG
C20orf133, exon 8 reverse	GGC TCA ATG ACT AGG TGT AGT TGA T
C20orf133, exon 9 forward	TTT GTT CTA CGG CTA TGT CCT G
C20orf133, exon 9 reverse	AGT GAC GGC TCC ACT TCT TC
C20orf133, exon 10 forward	CCA TCT GGA ACA TTC TTG TGT TT
C20orf133, exon 10 reverse	GCA ACT GCA ATA GCC TTA AGT GT
C20orf133, exon 11 forward	TAA TTT CAG TGC TGC ATA TTA GCC
C20orf133, exon 11 reverse	GGC AAA CTG TTA CAG GGC AGA
C20orf133, exon 12 forward	CAT GCT TTC TTT GGT GGA GAG
C20orf133, exon 12 reverse	GGC TGT AAA GAG CAG AAC TGA TT
C20orf133, exon 13 forward	CTA TCA TGT TAG TGC TGA AAG CTG C
C20orf133, exon 13 reverse	TAA ATG AAG CCA GCC TGG CA
C20orf133, exon 14 forward	ATT AAA GCA CGG TTT CTG AAG G
C20orf133, exon 14 reverse	CAC TCA GGG TTG TTT TAG TTG GA
C20orf133, exon 15 forward	TCC AAC TAA AAC AAC CCT GAG TG
C20orf133, exon 15 reverse	CGA GTA TTT TCT TTT GCT ACT TCT AG
C20orf133, exon 16 forward	GAA TTT AAA AGG GCA ATG GAG GG
C20orf133, exon 16 reverse	TTT CCA TGG GCT CCA ATA GC
C20orf133, exon 17 forward	AAG ATA TTT CTG GGC CTA TGT GAG G
C20orf133, exon 17 reverse	AGC GTG TGC TGC TAT CTT CC
FLRT3, exon 1 forward	GAC ATC ACC CCC TTC TTC AG
FLRT3, exon 1 reverse	TGT CCC AGA AAG TTT GCT TG
FLRT3, exon 2 forward	GAG GTC AAC CTA TCC CTT CTG A
FLRT3, exon 2 reverse	TTG GAT AAT CCT GGA TGG GA
FLRT3, exon 3a forward*	GGG TTC TGA AGT AAC GGA AGC
FLRT3, exon 3a reverse*	TGG AAA CCT GTT GAA CAA TCA
FLRT3, exon 3b forward*	TCA CCA TCT CTT CAA GGT CTC A
FLRT3, exon 3b reverse*	TCT GTC ACC TCT GAT ACC ATT CA
FLRT3, exon 3c forward*	AAG GAT CAC CAA ACC ACA GG
FLRT3, exon 3c reverse*	ATG CTG AAG GAC TCA CAG CA
FLRT3, exon 3d forward*	CCG AAG CTA CAG AGA CAG TGG
FLRT3, exon 3d reverse*	TCT CCA TTT TTG CTC TAG GCA

**FLRT3* exon 3 was divided into 4 regions; a, b, c, and d.

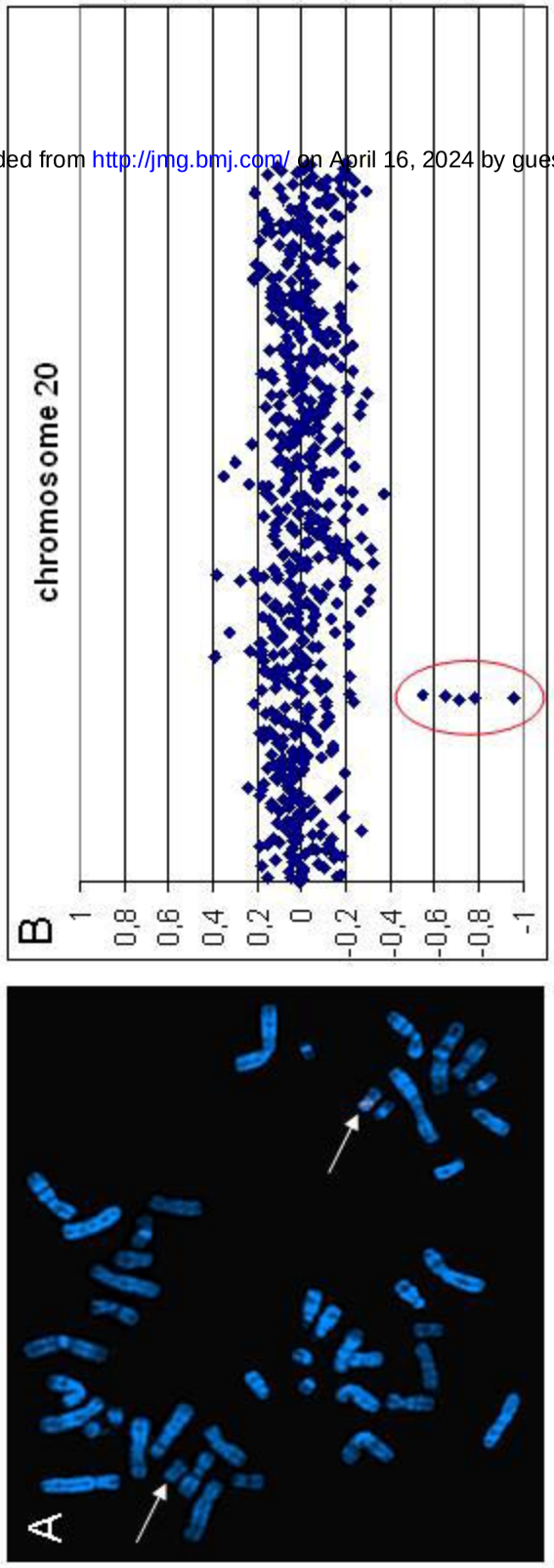

Figure 1

Figure 2A

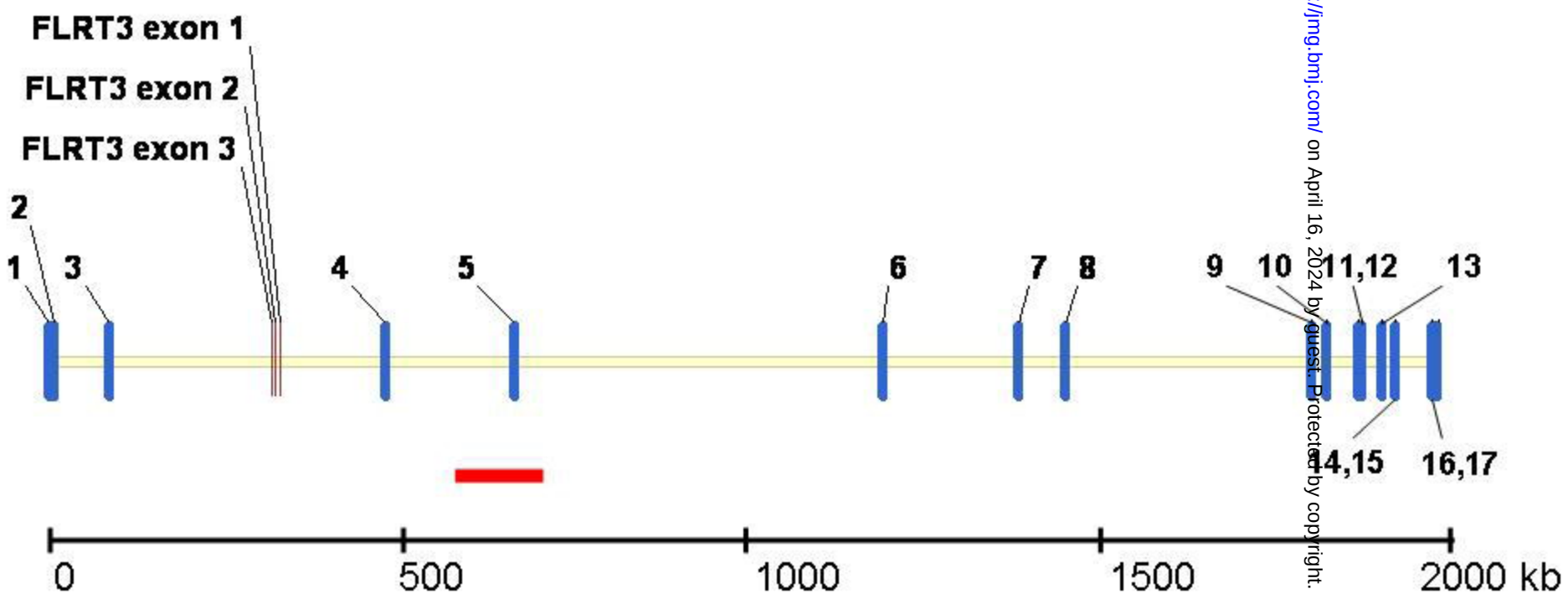

Figure 2B

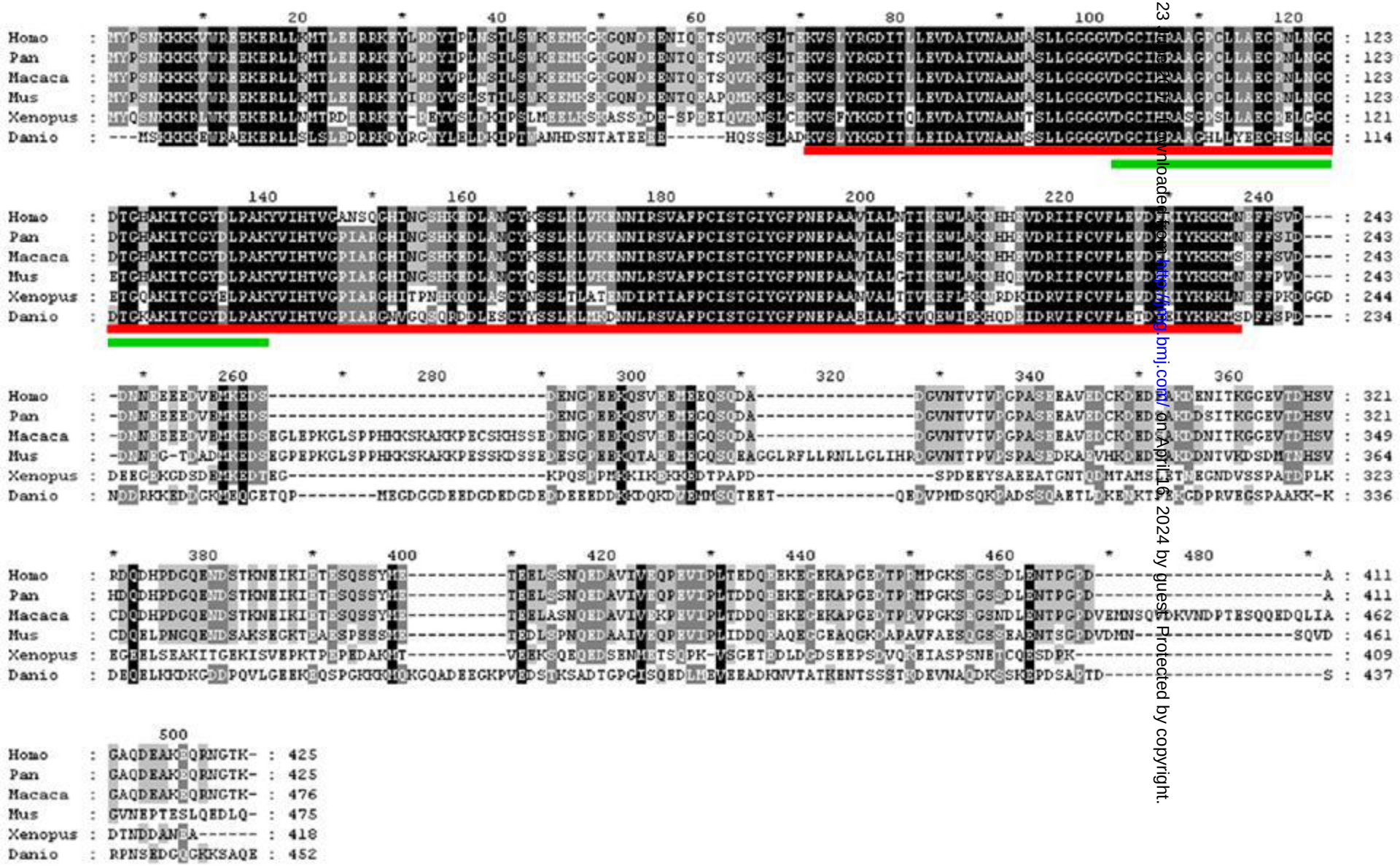

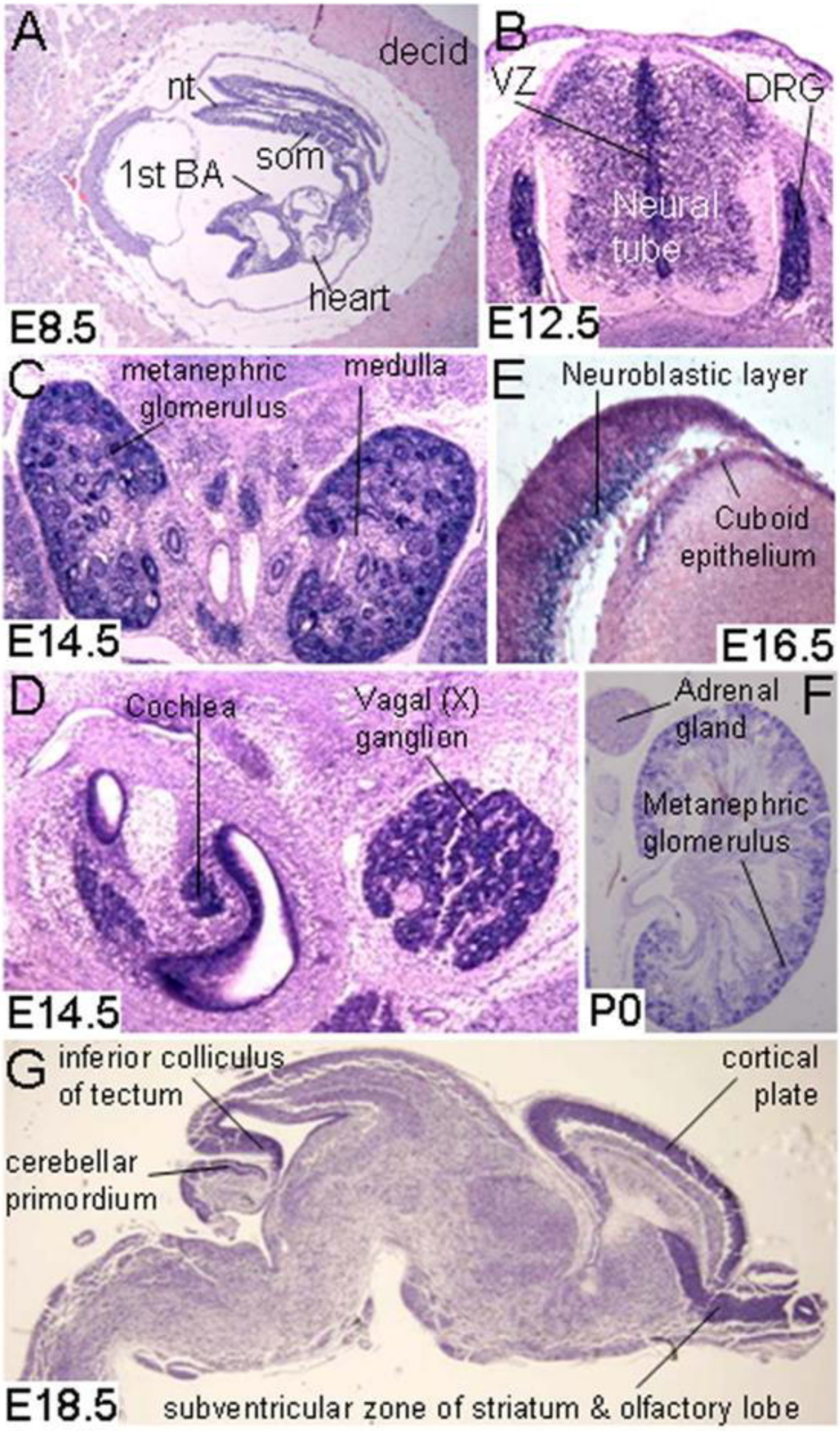
A
decid
nt
som
1st BA
heart
E8.5
B
VZ
DRG
Neural tube
E12.5
C
metanephric glomerulus
medulla
E14.5
E
Neuroblastic layer
Cuboid epithelium
E16.5
D
Cochlea
Vagal (X) ganglion
E14.5
F
Adrenal gland
Metanephric glomerulus
P0
G
inferior colliculus of tectum
cortical plate
cerebellar primordium
E18.5
subventricular zone of striatum & olfactory lobe

Figure 3